NASA TM X-56017

RESULTS OF A FEASIBILITY STUDY USING THE NEWTON-RAPHSON DIGITAL COMPUTER PROGRAM TO IDENTIFY LIFTING BODY DERIVATIVES FROM FLIGHT DATA

Alex G. Sim

(NASA-TH-X-56017) RESULTS OF A FEASIBILITY STUDY USING THE NEWTON-RAPHSON DIGITAL COMPUTER PROGRAM TO IDENTIFY LIFTING BODY DERIVATIVES FROM FLIGHT DATA (NASA) 41 p HC \$4.25 CSCL 01A

N74-11814

Unclas G3/01 23313

October 1973



NATIONAL AERONAUTICS AND SPACE ADMINISTRATION Washington, D. C. 20546

RESULTS OF A FEASIBILITY STUDY USING THE NEWTON-RAPHSON DIGITAL COMPUTER PROGRAM TO IDENTIFY LIFTING BODY DERIVATIVES FROM FLIGHT DATA

Alex G. Sim Flight Research Center

SUMMARY

A brief study was made to assess the applicability of the Newton-Raphson digital computer program as a routine technique for extracting aerodynamic derivatives from flight tests of lifting body types of vehicles. Lateral-directional flight data from flight tests of the HL-10 lifting body research vehicle were utilized. The results, in general, show the computer program to be a reliable and expedient means for extracting derivatives for this class of vehicle as a standard procedure. This result was true even when stability augmentation was used. An "a priori" weighting option available in the computer program was found to be a desirable feature. As a result of the study, a credible set of HL-10 lateral-directional derivatives was obtained from flight data. These derivatives are compared with results from wind-tunnel tests.

INTRODUCTION

Prior to the start of the M2-F3 lifting body research vehicle flight program (ref. 1), the need existed for assessing the reliability of using the Newton-Raphson digital computer program (refs. 2 to 4) as the principal means of derivative extraction for future lifting body flight tests. A feasibility study was therefore conducted in which previously obtained lateral-directional flight data of the HL-10 lifting body were used. This vehicle was chosen because it was well documented in terms of wind-tunnel studies (ref. 5) and earlier flight evaluations of its stability and control characteristics (ref. 6). In addition, time histories of transient maneuvers were readily available in digitized form.

Two ground rules were used to conduct this study. First, various options available in the computer program were held fixed, and, second, once these options were established, each maneuver was run one time only. These rules were established to ascertain whether an acce. able set of flight derivatives could be obtained by using only one computer run per maneuver.

The resulting set of HL-10 lateral-directional derivatives obtained is presented and

compared with wind-tunnel data of reference 5. In addition, the effects of using the computer program a priori option are included.

SYMBOLS

Derivatives are presented as standard NASA coefficients of forces and moments. A right-hand sign convention is used to determine the direction of all forces, moments, angular displacements, and velocity.

Physical quantities are given in both the International System of Units (SI) and parenthetically in U.S. Customary Units. All measurements were taken in U.S. Customary Units. Conversion factors can be found in reference 7.

A	stability matrix, P × P
^{a}y	transverse acceleration, g
В	control matrix, $P \times Q$
b	reference body span, m (ft)
C	transformation matrix, P × P
$\overline{\mathbf{F}}$	force, N (lb)
G	partition of matrix relating the state vector to the observation vector, $(R-P) \times P$
g	acceleration due to gravity, 9.8 m/sec ² (32.2 ft/sec ²)
н	partition of matrix relating the control vector to the observation vector, $(R - P) \times Q$
I	identity matrix
$^{\mathrm{I}}\mathbf{x}$	rolling moment of inertia, kg-m ² (slug-ft ²)
I _{XZ}	product of inertia, kg-m ² (slug-ft ²)
$^{\mathrm{I}}\mathrm{_{Z}}$	yawing moment of inertia, kg-m ² (slug-ft ²)
M	Mach number
$\overline{\mathbf{M}}$	moment, m-N (ft-lb)
m	mass, kg (slugs)
О	null matrix

P	number of state variables
p	rolling rate, rad/sec or deg/sec
Q	number of control variables
ā	dynamic pressure, N/m^2 (lb/ft ²)
R	number of observation variables
r	yawing rate, rad/sec or deg/sec
S	reference planform area, m ² (ft ²)
<u>u</u>	control vector (Q × 1)
v	velocity, m/sec (ft/sec)
x	X-axis
<u>x</u>	state vector, $P \times 1$
Y	Y-axis
<u>Y</u>	observation vector, $\mathbf{R} \times 1$
Z	Z-axis
α	angle of attack, deg
β	angle of sideslip, deg
ôa	aileron deflection, deg
$\delta_{\mathbf{r}}$	rudder deflection, deg
δ ₀	constant control deflection, rad or deg
heta	pitching attitude, deg
$oldsymbol{arphi}$	angle of bank, deg
\mathbf{c}_{l}	rolling-moment coefficient, qSb
C _n	yawing-moment coefficient, $\frac{\overline{M}_X}{\overline{qSb}}$
$c_{\mathbf{v}}$	side-force coefficient, \overline{q} S

$$\begin{split} \mathbf{L}_{\beta} &= \frac{\bar{\mathbf{q}}\mathbf{S}\mathbf{b}}{\mathbf{I}_{\mathbf{X}}} & \mathbf{C}_{l_{\beta}} \\ \mathbf{N}_{\beta} &= \frac{\bar{\mathbf{q}}\mathbf{S}\mathbf{b}}{\mathbf{I}_{\mathbf{Z}}} & \mathbf{C}_{\mathbf{n}_{\beta}} \\ \mathbf{N}_{\beta} &= \frac{\bar{\mathbf{q}}\mathbf{S}\mathbf{b}}{\mathbf{I}_{\mathbf{Z}}} & \mathbf{C}_{\mathbf{n}_{\beta}} \\ \mathbf{N}_{\delta_{\mathbf{a}}}, \delta_{\mathbf{r}} &= \frac{\bar{\mathbf{q}}\mathbf{S}\mathbf{b}}{\mathbf{I}_{\mathbf{Z}}} & \mathbf{C}_{\mathbf{n}_{\delta_{\mathbf{a}}}, \delta_{\mathbf{r}}} \\ \mathbf{Y}_{\beta} &= \frac{\bar{\mathbf{q}}\mathbf{S}}{\mathbf{m}\mathbf{V}} & \mathbf{Y}_{\delta_{\mathbf{a}}}, \delta_{\mathbf{r}} &= \frac{\bar{\mathbf{q}}\mathbf{S}\mathbf{b}}{\mathbf{I}_{\mathbf{Z}}} & \mathbf{C}_{\mathbf{n}_{\delta_{\mathbf{a}}}, \delta_{\mathbf{r}}} \\ \mathbf{L}_{\mathbf{p}} &= \frac{\bar{\mathbf{q}}\mathbf{S}\mathbf{b}^{2}}{2\mathbf{V}\mathbf{I}_{\mathbf{X}}} & \mathbf{C}_{l_{\mathbf{p}}} \\ \mathbf{N}_{\mathbf{p}} &= \frac{\bar{\mathbf{q}}\mathbf{S}\mathbf{b}^{2}}{2\mathbf{V}\mathbf{I}_{\mathbf{Z}}} & \mathbf{C}_{\mathbf{n}_{\mathbf{p}}} \\ \mathbf{N}_{\mathbf{p}} &= \frac{\bar{\mathbf{q}}\mathbf{S}\mathbf{b}^{2}}{2\mathbf{V}\mathbf{I}_{\mathbf{Z}}} & \mathbf{C}_{\mathbf{n}_{\mathbf{p}}} \end{split}$$

Subscripts:

 $Y_p = \sin \alpha$

X X-axis component
Y Y-axis component
Z Z-axis component $\delta_a, \delta_r, \delta_o, p, r, \beta$ partial differentiation with respect to subscripted variable

A dot over a symbol signifies a derivative with respect to time.

METHOD OF ANALYSIS

A digital computer program was used to identify lateral-directional sets of derivatives from flight data. This program uses a modification of the Newton-Raphson method and is commonly called the Newton-Raphson program. Detailed discussion of the program, including theory and applications, is given in references 2 to 4. The appendix contains the set of equations (model) used to identify the derivatives for this report.

The method is an iterative technique which usually takes from three to six iterations to converge to a final set of derivatives. Basically, the program simultaneously changes all derivatives to minimize the difference between computed and measured time histories. The output time histories are assumed to contain noise, but the input (control) time

histories are defined as being noise free. The input time histories used were those for the ailerons (differential elevons) and rudder. The output time histories were those for roil rate, yaw rate, sideslip angle, bank angle, and lateral acceleration.

An option used, called "a priori" (ref. 2), allowed the starting set of derivatives to be weighed, which tended to hold the resulting derivatives near their starting value if no information about them was contained in the maneuver. The procedure used is to include a penalty for departure from the assumed starting value. For this study, wind-tunnel predictions were used as starting values.

DESCRIPTION OF VEHICLE

The HL-10 is a research vehicle of the lifting body class. Its basic aerodynamic shape is that of a thick, 74 sweep, delta planform with negative camber and three aft vertical fins. Pertinent physical characteristics are presented in table 1, and a three-view drawing is shown in figure 1.

The primary controls consisted of elevons and a rudder. The elevons provided both pitch and roll control, damping augmentation, and trim control. The rudder, located on the center vertical fin, was split so as to be operated both as a rudder and a speed brake. Secondary control surfaces were located on the inboard and outboard trailing edges of the tip fins and upper surfaces of the elevons. These surfaces served as two-position flaps and were deployed either open for transonic flight or closed for subsonic flight.

The primary control surfaces were actuated by irreversible hydraulic systems and accepted commands from both the pilot and the stability augmentation system (SAS). The SAS consisted of a three-axis rate feedback system with pilot adjustable gains.

Further vehicle description can be found in references 6, 8, 9, and 10.

INSTRUMENTATION

Conventional NASA instrumentation was used to determine all flight quantities of interest (ref. 6). Data were acquired by means of a 9-bit pulse code modulation system and were telemetered in real time to a ground station. Measurement accuracies of these quantities are detailed in reference 6.

FLIGHT TESTS

Procedures

Frequent weight and balance measurements were made to verify the location of the vehicle center of gravity. Moments of inertia were determined experimentally before the initial flight by means of an inertia swing (ref. 11). The inertia estimate was updated analytically whenever the mass distribution changed.

Like other lifting bodies, the HL-10 vehicle was air-launched from a modified B-52

airplane at an altitude of approximately 14,000 meters (45,000 feet) and a Mach number of 0.67. After launch, the pilot flew a preplanned flight profile. The unpowered, or glide, flights lasted less than 4 minutes and were usually made below a Mach number of 0.7. For powered flights, the engine was lit immediately after launch, angle of attack was increased to gain altitude, and then the vehicle was pushed over to increase Mach number. The powered portion of the flight, which usually lasted from 90 seconds to 180 seconds, was made in the transonic configuration. A change to the subsonic configuration was made when the Mach number decreased to about 0.7. The altitude at this time was about 9150 meters (30,000 feet). Most of the stability and control data were obtained after engine burnout.

In general, maneuvers from which data were obtained were performed at altitudes above approximately 6100 meters (20,000 feet) to provide the pilot with enough time to set up for the final approach and landing. The trajectories flown precluded steady flight conditions. In addition, the SAS was generally used throughout the flight profile.

MANEUVERS

The maneuvers used had previously been performed for the purpose of analog derivative extraction (ref. 6). These were the standard doublet types of maneuvers which have been used (ref. 8) to excite the airplane's transient characteristics. The SAS was generally used to insure satisfactory handling qualities during maneuvers. However, damper gains were usually at or less than 0.5 deg/deg/sec. All maneuvers used in this study were performed with the vehicle in the transonic configuration. Control derivatives obtained from a maneuver were used only if the maneuver contained a pilot input from that control.

RESULTS AND DISCUSSION

Summary of Results

For this study an attempt was made to analyze 42 lateral-directional maneuvers (i.e., all that were available in convenient digitized form). Acceptable sets of derivatives were obtained in 26 cases. Of the maneuvers which yielded unacceptable results, 13 converged to a set of derivatives with an unacceptable fit error, while three were not convergent. Of the 13 convergent cases, two cont. Led atmospheric turbulence, seven were very weak in amplitude, and the remaining four were of very large amplitude. It should be noted that four of the unacceptable cases were later found to give acceptable results after changes were made in the program options. To follow the ground rules and keep the study consistent, these four cases are not presented.

Figures 2, 3, and 4 present time histories of the typical, best, and worst (but still acceptable) matches obtained.

Comparison of Flight and Wind-Tunnel Data

Figures 5 to 9 compare the flight derivatives with wind-tunnel predictions. All

derivatives are plotted as functions of angle of attack at selected wind-tunnel test Mach numbers. Wind-tunnel values are based on data from reference 5.

An overview of figures 5 to 9 indicates that the effective dihedral derivative, $C_{l_{\beta}}$, and the directional stability derivative, $C_{n_{\beta}}$, agree well with wind-tunnel data. The side-force derivative, $C_{Y_{\beta}}$, is often lower than wind-tunnel predictions. Aileron control derivatives are approximately at the same level as wind-tunnel data. However, at a Mach number of 1.2 (fig. 8) is more proverse than wind-tunnel predictions at high angles of attack. The side force due to aileron, $C_{Y_{\delta}}$, from flight was not determined (i.e., held fixed) in this study. The rudder effectiveness, $C_{n_{\delta}}$, substantiated wind-tunnel predictions. The rolling moment due to rudder, $C_{l_{\delta}}$, was approximately at the same level as wind-tunnel data, although it tended to have a good deal of scatter, indicating that it was relatively hard to identify. The side force due to rudder, $C_{Y_{\delta}}$, was consistently lower than the wind-tunnel data.

Damping derivatives are generally more difficult to identify than other derivatives because of their small magnitude and the use of the SAS during transient maneuvers. The damping derivatives $\begin{pmatrix} C_l & C_l & C_n \\ p & r \end{pmatrix}$, and $\begin{pmatrix} C_n & S_n \\ r \end{pmatrix}$ show enough scatter to support this.

Effect of the A Priori Option

Figure 10 compares the derivatives obtained from flight data with and without the a priori option for a Mach number of 1.2. The general level of the major parameters $(C_{l_{\beta}}, C_{n_{\beta}}, C_{l_{\delta}}, C_{n_{\delta}}, C_{l_{\delta}}, and C_{n_{\delta}})$ is not significantly affected by using the option.

Scatter in the damping derivatives $(C_{j_{p}}, C_{n_{p}}, C_{l_{r}}, and C_{n_{r}})$ has been reduced,

although there is too much scatter in these derivatives obtained without a priori to determine it those with a priori were biased. The weighting on $C_{Y_{\vec{\rho}}}$ appears to be too high, such that this derivative was biased toward the wind-tunnel value.

It has been found that the option tends to help convergence--especially when the maneuver does not contain sufficient information to define all the derivatives well. The option was most successfully used to obtain derivatives from maneuvers with stability augmentation and maneuvers with weak pilot control inputs.

CONCLUDING REMARKS

A study was made of the feasibility of using the Newton-Raphson digital computer program to identify lifting body derivatives from flight data. The study showed that the Newton-Raphson program was a reliable and expedient means of extracting these derivatives on a routine basis. This was true even when stability augmentation was used. The a priori option was shown to be a desirable feature.

In general, a satisfactory set of HL-10 lifting body lateral-directional derivatives was obtained from the flight data.

Flight Research Center

National Aeronautics and Space Administration
Edwards, Calif., November 2, 1973

APPENDIX

EQUATIONS OF MOTION MECHANIZED IN THE NEWTON-RAPHSON DIGITAL COMPUTER PROGRAM

The following state equations were used in the basic model for this study:

$$C\underline{\dot{x}} = A\underline{x} + B\underline{u}$$

$$\underline{\mathbf{y}} = \begin{bmatrix} \underline{\mathbf{I}} \\ \mathbf{G} \end{bmatrix} \underline{\mathbf{x}} + \begin{bmatrix} \underline{\mathbf{O}} \\ \mathbf{H} \end{bmatrix} \underline{\mathbf{u}}$$

where \underline{x} , $\underline{\dot{x}}$, \underline{u} , and \underline{y} are time varying.

For the lateral-directional mechanization,

$$\underline{\mathbf{x}} = \begin{bmatrix} \mathbf{p} \\ \mathbf{r} \\ \beta \\ \varphi \end{bmatrix} \qquad \underline{\mathbf{u}} = \begin{bmatrix} \delta_{\mathbf{a}} \\ \delta_{\mathbf{r}} \\ \delta_{\mathbf{1}} \\ 1 \end{bmatrix} \qquad \mathbf{y} = \begin{bmatrix} \mathbf{r} \\ \beta \\ \dot{\mathbf{p}} \\ \dot{\mathbf{r}} \\ \dot{\mathbf{a}} \end{bmatrix}$$

$$\mathbf{A} = \begin{bmatrix} \mathbf{L}_{\mathbf{p}} & \mathbf{L}_{\mathbf{r}} & \mathbf{L}_{\beta} & 0 \\ \mathbf{N}_{\mathbf{p}} & \mathbf{N}_{\mathbf{r}} & \mathbf{N}_{\beta} & 0 \\ \mathbf{Y}_{\mathbf{p}} & -\cos(\alpha)^* & \mathbf{Y}_{\beta} & g/V\cos(\varphi)^* \\ 1^* & \tan(\theta)^* & 0 & 0 \end{bmatrix}$$

^{*}Normally held fixed.

$$\mathbf{B} = \begin{bmatrix} \mathbf{L}_{\delta_{\mathbf{a}}} & \mathbf{L}_{\delta_{\mathbf{r}}} & \mathbf{L}_{\delta_{\mathbf{0}}} \\ \mathbf{N}_{\delta_{\mathbf{a}}} & \mathbf{N}_{\delta_{\mathbf{r}}} & \mathbf{N}_{\delta_{\mathbf{0}}} \\ \mathbf{Y}_{\delta_{\mathbf{a}}}^{*} & \mathbf{Y}_{\delta_{\mathbf{r}}} & \mathbf{Y}_{\delta_{\mathbf{0}}} \\ \mathbf{0} & \mathbf{0} & \mathbf{0} \end{bmatrix}$$

$$G = \begin{bmatrix} L_{\mathbf{p}} & L_{\mathbf{r}} & L_{\beta} & 0 \\ N_{\mathbf{p}} & N_{\mathbf{r}} & N_{\beta} & 0 \\ 0 & 0 & Y_{\beta} & 0 \end{bmatrix}$$

$$\mathbf{H} = \begin{bmatrix} \mathbf{L}_{\delta_{\mathbf{a}}} & & \mathbf{L}_{\delta_{\mathbf{r}}} & & \mathbf{L}_{\delta_{\mathbf{0}}} \\ \mathbf{N}_{\delta_{\mathbf{a}}} & & \mathbf{N}_{\delta_{\mathbf{r}}} & & \mathbf{N}_{\delta_{\mathbf{0}}} \\ \mathbf{Y}_{\delta_{\mathbf{a}}} & & \mathbf{Y}_{\delta_{\mathbf{r}}} & & \mathbf{Y}_{\delta_{\mathbf{0}}} \end{bmatrix}$$

REFERENCES

- 1. Sim, Alex G.: Flight-Determined Stability and Control Characteristics of the M2-F3 Lifting Body. NASA TN D-7511, 1973.
- 2. Iliff, Kerneth W.; and Taylor, Lawrence W., Jr.: Determination of Stability Derivatives From Flight Data Using a Newton-Raphson Minimization Technique. NASA TN D-6579, 1972.
- 3. Taylor, Lawrence W., Jr.; and Iliff, Kenneth W.: Systems Identification Using a Modified Newton-Raphson Method A Fortran Program. NASA TN D-6734, 1972.
- 4. Wolowicz, Chester H.; Iliff, Kenneth W.; and Gilyard, Glenn B.: Flight Test Experience in Aircraft Parameter Identification. AGARD CP-119, Nov. 1972, pp. 23-1 23-13.
- 5. Ladson, Charles L.; and Hill, Acquilla S.: Aerodynamics of a Model of the HL-10 Flight-Test Vehicle at Mach 0.35 to 1.80. NASA TN D-6018, 1971.
- 6. Strutz, Larry W.: Flight-Determined Derivatives and Dynamic Characteristics for the HL-10 Lifting Body Vehicle at Subsonic and Transonic Mach Numbers. NASA TN D-6934, 1972.
- 7. Mechtly, E. A.: The International System of Units. Physical Constants and Conversion Factors. Second Revision. NASA SP-7012, 1973.
- E. Painter, Weneth D.; and Sitterle, George J.: HL-10 Lifting Body Flight Control System Characteristics and Operational Experience. NASA TM X-2956, 1973.
- 9. Kempel, Robert W.; and Manke, John A.: Flight Evaluation of the HL-10 Lifting Body Handling Qualities at Mach Numbers From 0.30 to 1.86. NASA TN D-7537, 1973.
- 10. Kempel, Robert W.; Strutz, Larry W.; and Kirsten, Paul W.: Stability and Control Derivatives of the Lifting Body Vehicles. Flight Test Results Pertaining to the Space Shuttlecraft. NASA TM X-2101, 1970, pp. 11-27.
- 11. Boucher, Robert W.; Rich, Drexel A.; Crane, Harold L.; and Matheny, Cloyce E.: A Method for Measuring the Product of Inertia and the Inclination of the Principal Longitudinal Axis of Inertia of an Airplane. NACA TN 3084, 1954.

TABLE 1. - PHYSICAL CHARACTERISTICS OF THE HL-10 LIFTING BODY VEHICLE

(a) Reference areas and lengths

Body - Reference planform area, m ² (ft ²))
Span, m (ft)	,
Aspect ratio, b ² /S	
Area, each, m^2 (ft ²)	!) })
Chord: Root, m (ft)	
Elevon flap (two) - Area, each, m^2 (ft ²)	0)
Area, each, m (ft)	
Root, m (ft)	
Vertical stabilizer - Area, m^2 (ft ²)	0)
Height, m (ft)	2)
Chord: Root, m (ft)	7)
Leading-edge sweep, deg	5
Area, each, m^2 (ft ²)	2)
Area, each, m^2 (ft ²)	
Chord perpendicular to hinge line, m (ft)	
Area, m ² (ft ²)	31)

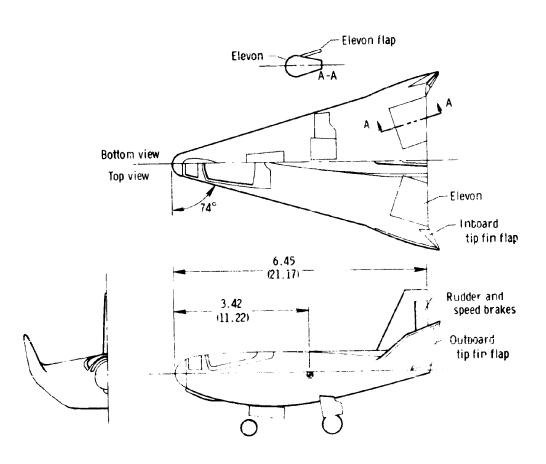


Figure 1. Three-view drawing of the HL-10 $\nu c^{\alpha} icle,$

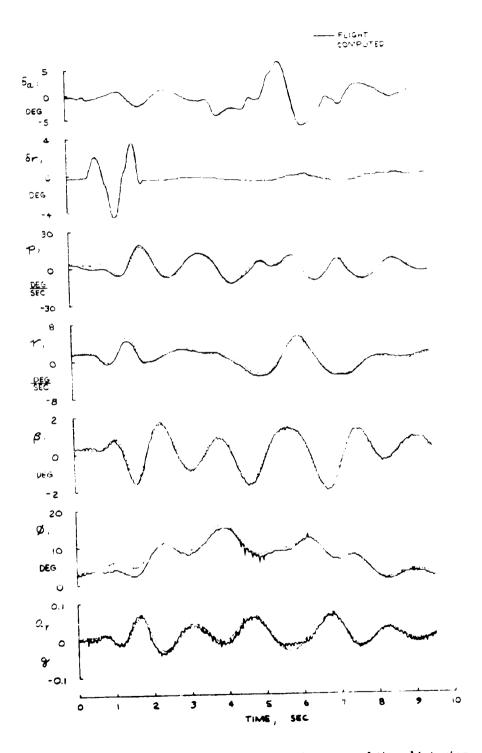


Figure 2. Typical comparison of the flight and computed time histories.

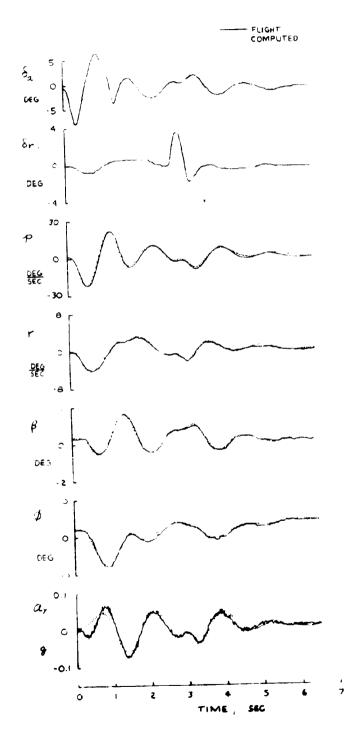


Figure 3 Best comparison obtained of the flight and computed time histories.

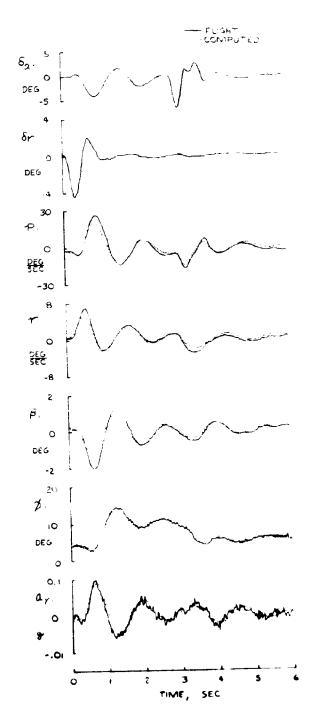


Figure 4. Worst comparison used of the flight and computed time histories.

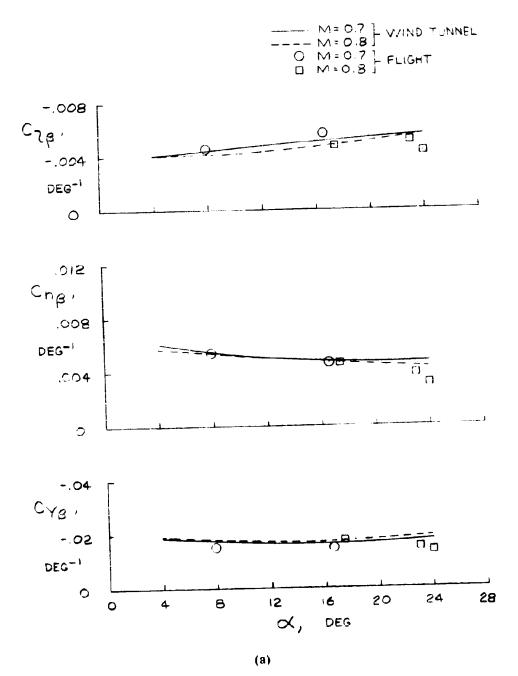


Figure ϕ . Comparison of derivatives obtained from flight data with wind-tunnel predictions for Mach numbers of 0.7 and 0.8.

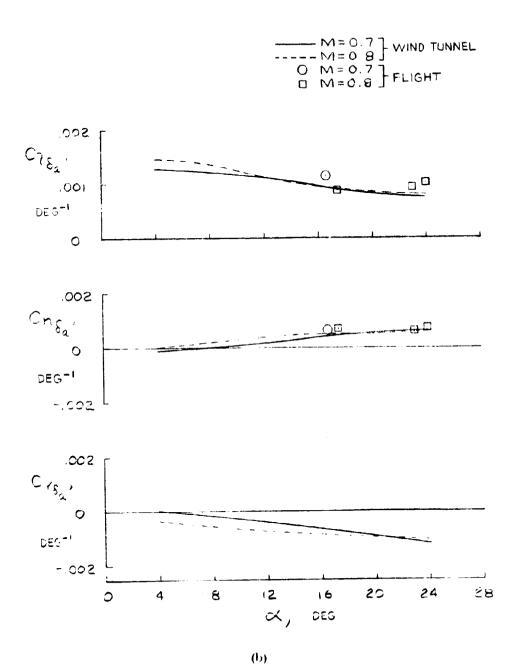


Figure 5. Continued.

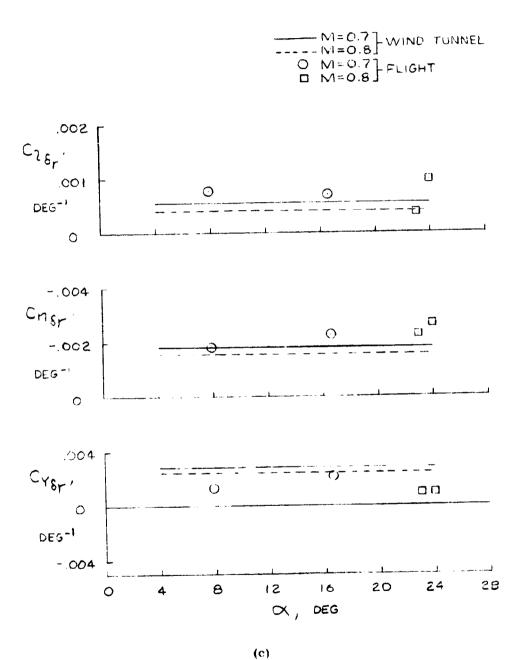


Figure 5. Continued

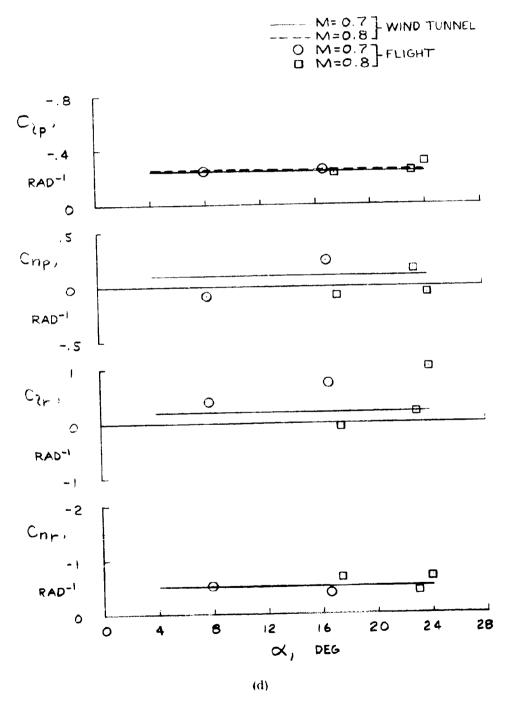


Figure 5. Concluded,



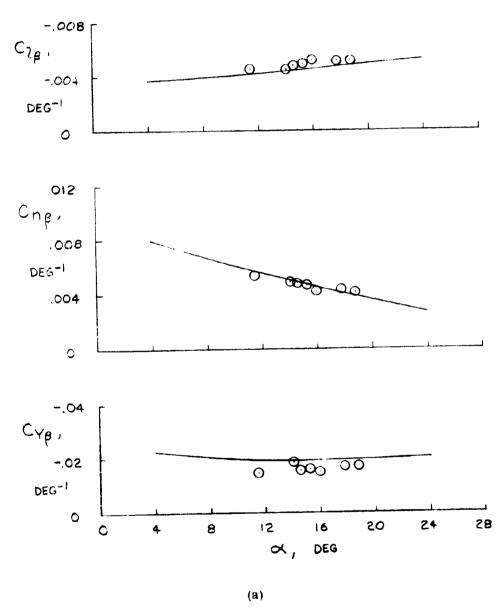


Figure 6 Comparison of derivatives btained from flight data with wind-tunnel predictions for a Mach number of 0, 9.



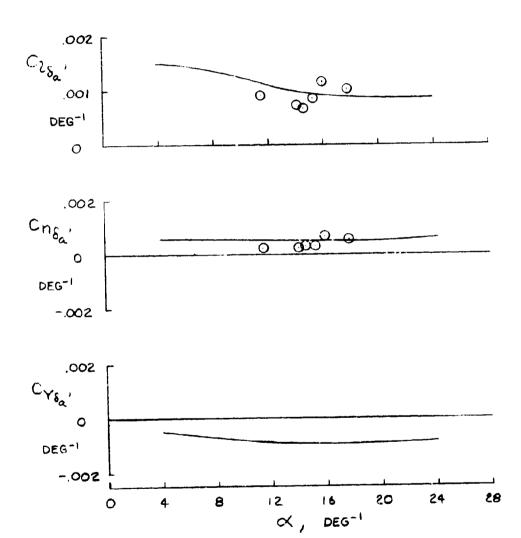
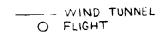


Figure 6. Continued.

(b)



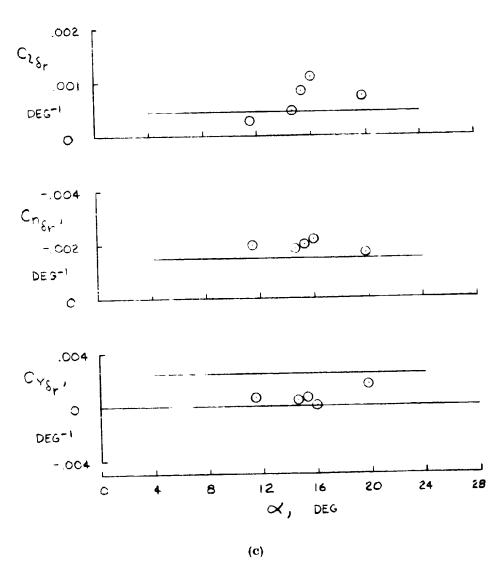


Figure 6. Continued.



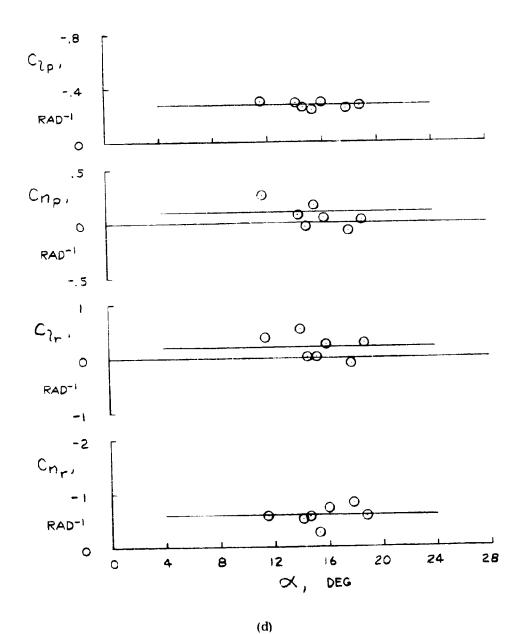


Figure 6. Concluded.

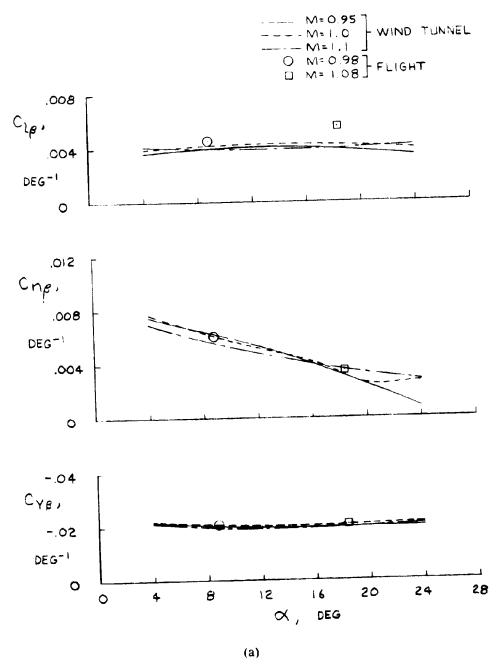


Figure 7. Comparison of derivatives obtained from flight data with wind-tunnel predictions for Mach numbers from 0.95 to 1.1.

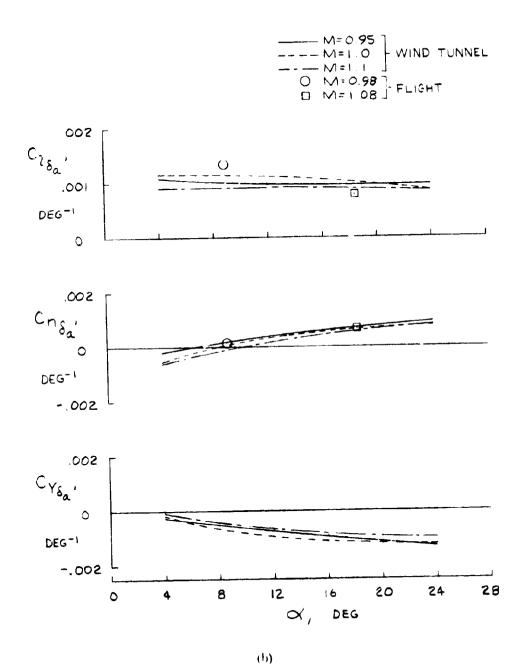
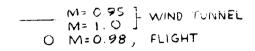
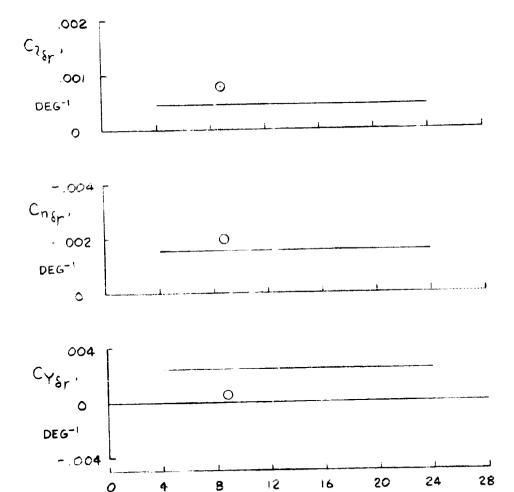


Figure 7. Continued.





(C)

∝, DEG

Figure 7. Continued,

0

4

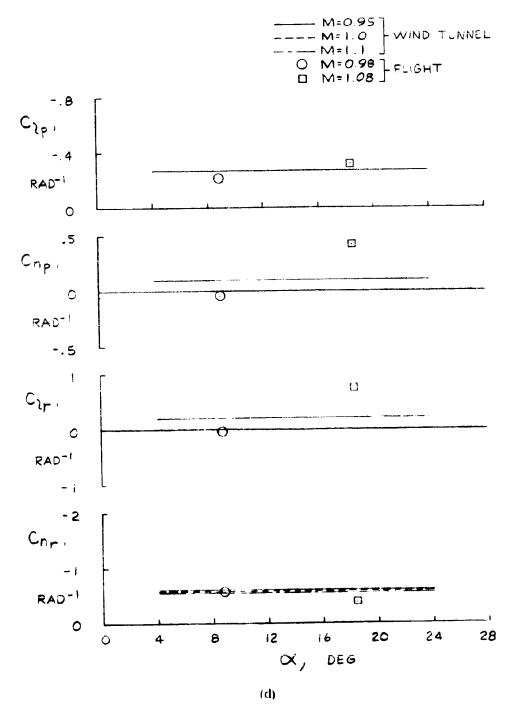


Figure 7. Concluded,

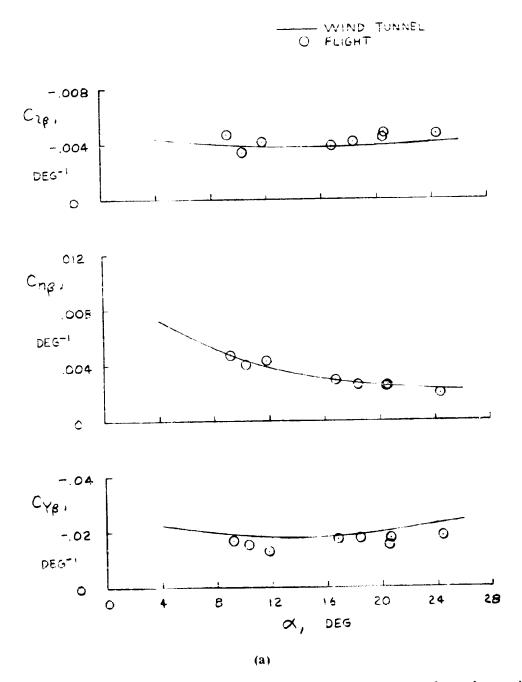
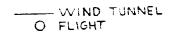


Figure 8. Comparison of derivatives obtained from flight data with wind-tunnel predictions for a Mach number of 1, 2.



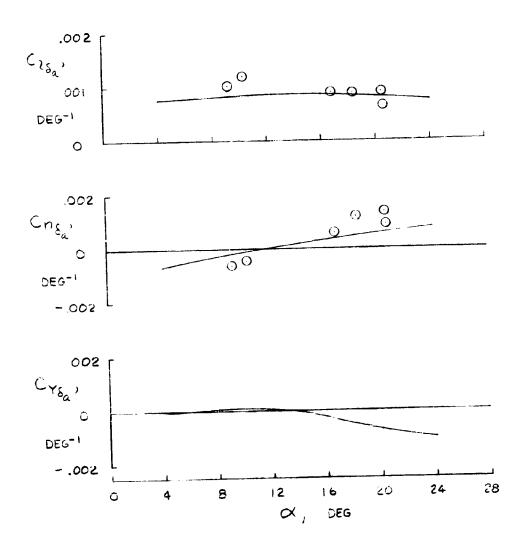


Figure 8. Continued.

(b)



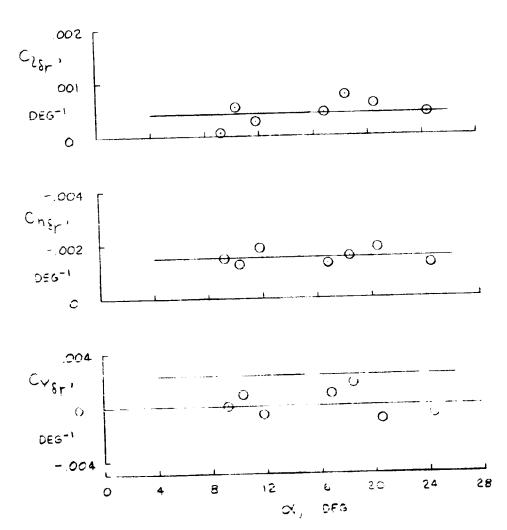


Figure 8. Continued

(c)



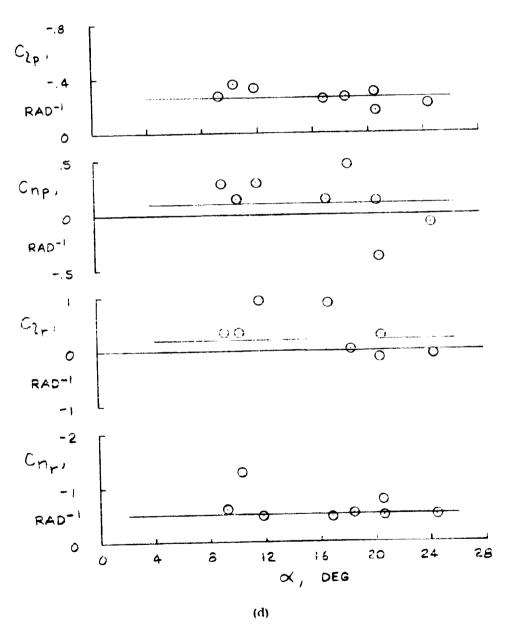


Figure 8. Concluded,

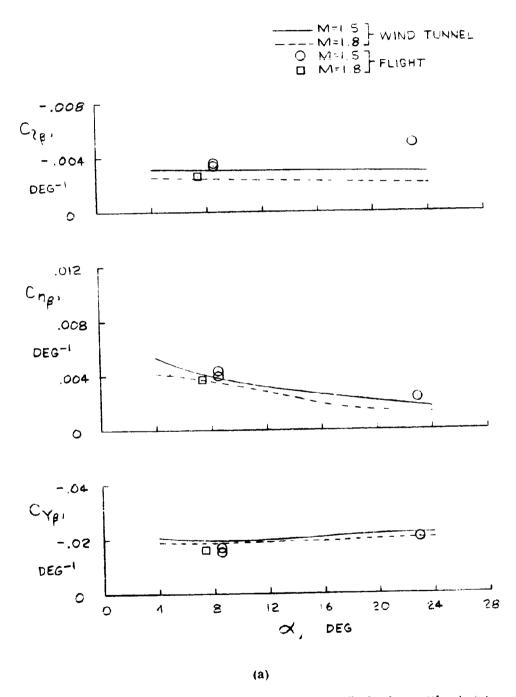
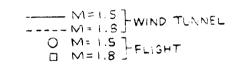
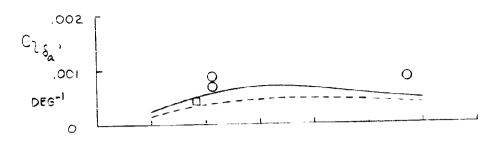
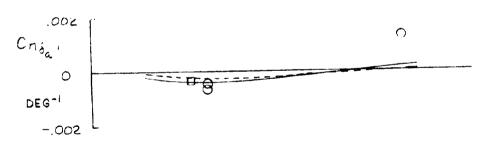


Figure 9 Comparison of derivatives obtained from flight data with wind-tunnel predictions for Mach numbers of 1, 5 and 1, 8.







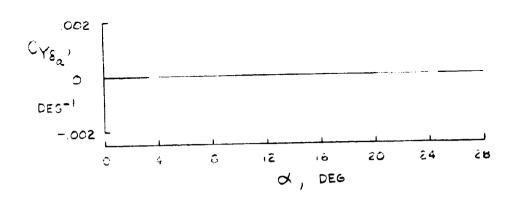
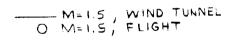


Figure 9. Continued.

(b)



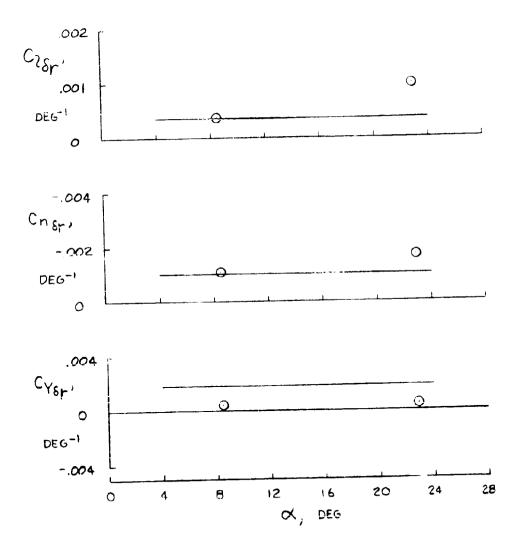


Figure 9. Continued.

(c)

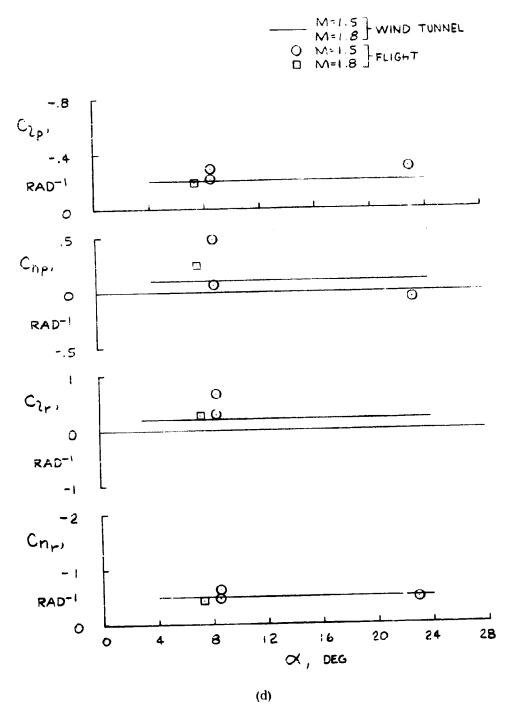
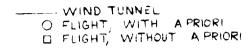


Figure 9. Concluded.



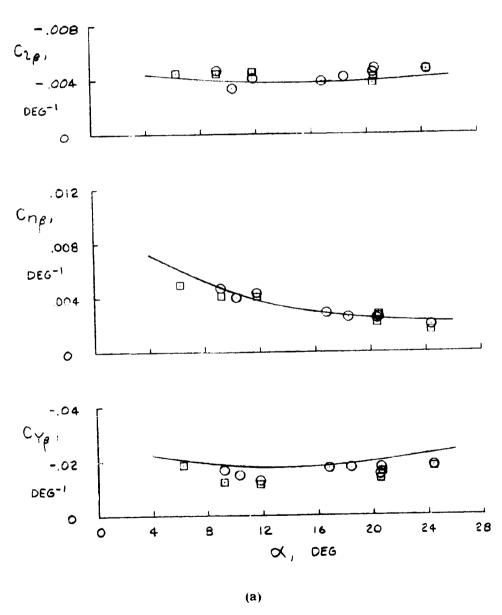


Figure 10. Comparison of derivatives obtained from flight data with and without the a priori option for a Mach number of 1.2.

WIND TUNNEL
O FLIGHT, WITH A PRIORI
FLIGHT, WITHOUT A PRIORI

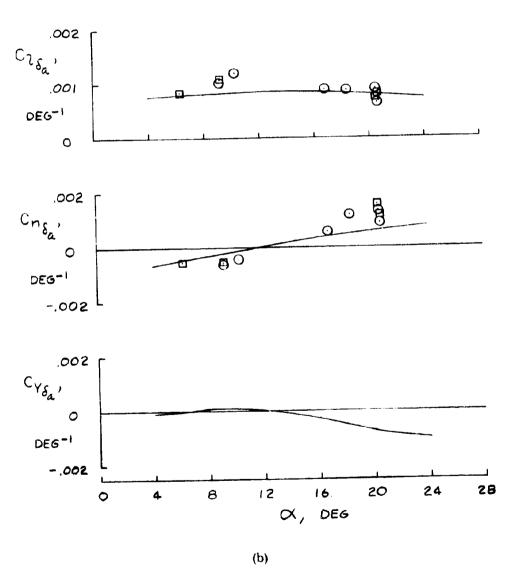


Figure 10. Continued.

WIND TUNNEL
O FLIGHT, WITH A PRIORI
O FLIGHT, WITHOUT A PRIORI

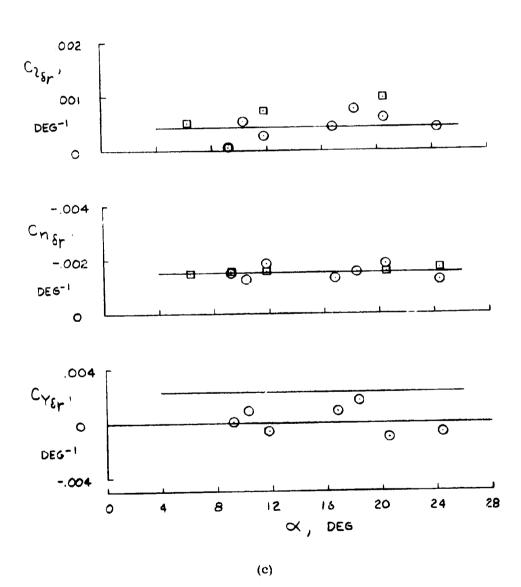
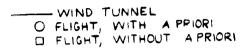


Figure 10. Continued.



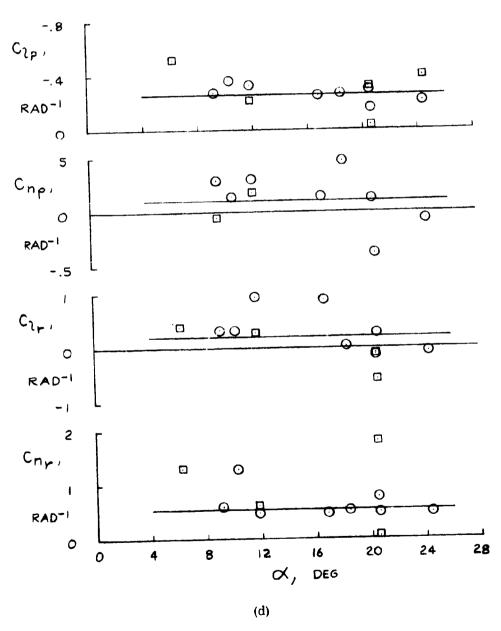


Figure 10. Concluded.